Economic Geology, v. 108, pp. 883–894

Re-Os DATING OF MOLYBDENITE WITHIN HEMATITE BRECCIAS FROM THE VULCAN Cu-Au PROSPECT, OLYMPIC Cu-Au PROVINCE, SOUTH AUSTRALIA

Anthony Reid,[1,†] Robert N. Smith,[2] Timothy Baker,[1,*] Elizabeth A. Jagodzinski,[1] David Selby,[3] Courtney J. Gregory,[4] and Roger G. Skirrow[5]

[1] *Geological Survey of South Australia, Department of Manufacturing Innovation Trade Resources and Energy, GPO Box 1264, Adelaide, South Australia, Australia*

[2] *Tasman Resources Ltd, Level 15, 197 St George's Tce, Perth, Western Australia 6000, Australia*

[3] *Department of Earth Sciences, University of Durham, Durham DH1 3LE, United Kingdom*

[4] *Department of Applied Geology, Curtin University of Technology, Western Australia 6845, Australia*

[5] *Minerals and Natural Hazards Division, Geoscience Australia, Symonston, ACT, Australia*

Abstract

The Vulcan prospect is a newly discovered Cu-Au prospect located within the eastern Gawler craton, South Australia. The prospect is entirely subsurface and defined by a geophysical anomaly intersected by diamond drilling. Eight drill holes have all intersected hematite-rich alteration and Cu-Au mineralization within a variety of breccia types ranging from those composed entirely of hydrothermal hematite + sericite + chlorite to those dominated by altered rock in which clasts of protolith rock are preserved. The highest-grade zones of mineralization at Vulcan occur within hematite-dominant breccias. Molybdenite within hematite-rich brecciated granite samples has been dated via the Re-Os method and yields a crystallization age of 1586 ± 8 Ma (including decay constant uncertainties). SHRIMP zircon U-Pb analyses show that a sample of hematite-sericite-chlorite–altered and brecciated granite was emplaced at 1743 ± 7 Ma. The new data from Vulcan confirm that hematite breccia-related Cu-Au mineralization formed during a widespread alteration and mineralization event between ca. 1600 and 1570 Ma, broadly coeval with the voluminous felsic large igneous province of the Gawler Range Volcanics/Hiltaba Suite, and are consistent with most interpretations of the geology of the Olympic Cu-Au province.

Introduction

The Olympic Dam iron oxide copper-gold (IOCG) deposit and the Prominent Hill, Carrapateena, and Hillside deposits all occur within a Cu-Au ± U–endowed metallogenic province that occupies some 600 km of strike length along the eastern margin of the Gawler craton, South Australia (Fig. 1). The concept that these deposits together with a host of smaller Cu-Au ± U prospects form part of a single metallogenic province, the Olympic Cu-Au province, developed out of investigations into the mineralogy, fluid composition, structural architecture, and geochronology of Cu-Au deposits across the eastern Gawler craton (Skirrow et al., 2002, 2007). One of the most important features of the notion of an "Olympic Cu-Au province" is that it considers all of the diverse alteration and mineralization styles found within this portion of the Gawler craton to be linked in some way to a lithospheric-scale magmatic-hydrothermal system that formed as a result of the bimodal but dominantly felsic A-type magmas of the ca. 1600 to 1570 Ma Gawler Range Volcanics and Hiltaba Suite (Flint et al., 1993). The majority of the available geochronology generally confirms that alteration and mineralization in this metallogenic province are broadly synchronous with this magmatic event (Table 1). Nevertheless, there are two important caveats: (1) the majority of the geochronology has been conducted on relatively high temperature minerals, such as titanite or garnet, and (2) there is very little geochronology from any of the major hematite breccia-style deposits, with the exception of Olympic Dam itself. Because a number of the Cu-Au prospects within the province, such as Emmie Bluff and Punt Hill, have been shown to have a paragenetic evolution from early high-temperature, magnetite-rich alteration to a lower-temperature, hematite-rich sericite-chlorite-carbonate alteration (Gow et al., 1994; Bastrakov et al., 2007; Skirrow et al., 2007), the possibility exists that the hematite-rich breccia systems could be part of a younger geologic event, since in the case of these two examples none of the dating has focused on the hematite end of the paragenetic spectrum. The one notable exception is the dating of sericite from the Torrens prospect (Skirrow et al., 2007), which the authors of that study suggested to record crystallization of sericite at 1575 ± 11 Ma during low-temperature alteration and which is within the interval of the Gawler Range Volcanics/Hiltaba Suite magmatic event.

The geochronology from Olympic Dam is, however, perhaps not as straightforward to interpret. Geochronology using a number of different isotopic decay systems from Olympic Dam gives a range of ages (Table 1). Early Rb-Sr dating gave a series of ages ranging from ca. 1520 to ca. 750 Ma (Reeve et al., 1990), whereas ion probe U-Pb dating of pitchblende gave discordant data with a maximum age of about 1400 Ma, which was suggested to represent a minimum age only (Reed et al., 1988). Whole-rock and sulfide Sm-Nd data gave an isochron age of 1572 ± 99 Ma (Johnson and McCulloch, 1995), although the age is very imprecise. Re-Os dating using whole rock and mineral separates gave a range of ages, from 3418 Ma to 672 Ma, with a poorly fitting isochron age of 1258 ± 28

† Corresponding author: e-mail, anthony.reid@sa.gov.au

* Present address: Eldorado Gold Corporation, 1188 Bentall 5-550 Burrard Street, Vancouver, BC V6C 2B5, Canada.

Submitted: June 28, 2012
Accepted: July 19, 2012

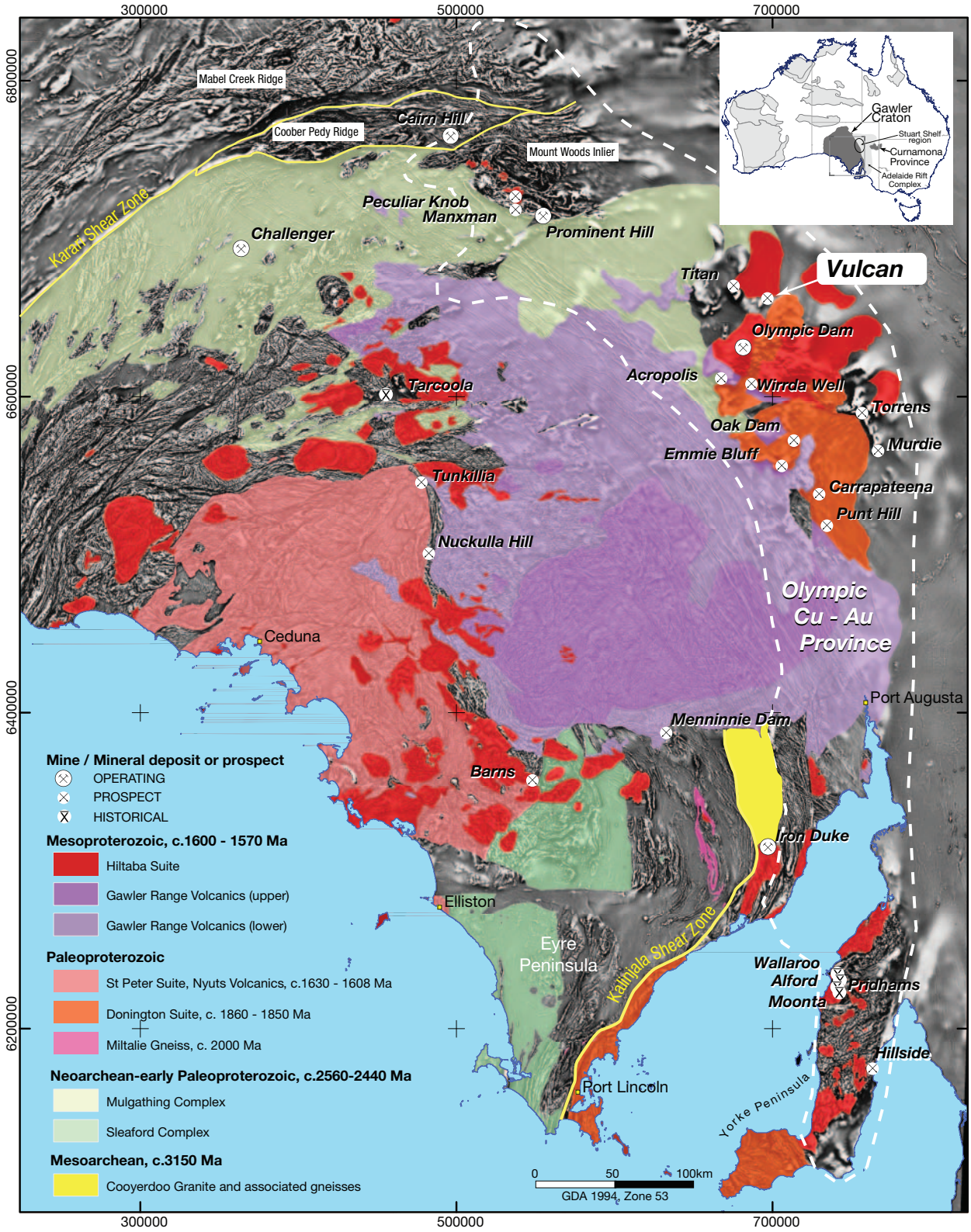

FIG. 1. Location of the Olympic Cu-Au province within the eastern Gawler craton, South Australia. Interpreted pre-Neoproterozoic solid geology, modified from Fairclough et al. (2003), is overlain on a first vertical derivative total magnetic intensity image (DMITRE data). Regions not colored within the Gawler craton are undifferentiated, predominantly Paleoproterozoic rocks. Also shown are the locations of the deposits and prospects across the region. Inset shows the location of the Gawler craton in the context of the outlines of major Archean-Proterozoic terranes of Australia. Also indicated is the approximate location of the Stuart shelf; the platform sediments are equivalent in age to sediments within the Adelaide Rift Complex.

Ma interpreted to represent a period of isotopic resetting rather than the time of primary mineralization (McInnes et al., 2008). Zircon U-Pb dating from Olympic Dam has constrained the age of the host 1595 ± 11 Ma Roxby Downs Granite (Johnson, 1993), and fragmented felsic dikes within the deposit have ages of 1592 ± 8 Ma, 1584 ± 20 Ma, and 1596 ± 4.4 Ma (Johnson and Cross, 1995; Jagodzinski, 2005). Two of these dikes were interpreted by Johnson and Cross (1995) to be peperites emplaced into unconsolidated hematite-altered breccias and, therefore, to constrain the timing of hematite alteration and brecciation. Recently, however, McPhie et al. (2011) have suggested that ragged and amoeboid shapes of felsic volcanic fragments within polymict breccias may be a result of brittle failure and hydrothermal replacement of preexisting volcanic material. If this is the case, then the zircon U-Pb emplacement ages of the felsic dikes dated by Johnson and Cross (1995) potentially provide only a maximum age constraint on the timing of mineralization. Therefore, as there remains an element of doubt over the age of mineralization at Olympic Dam, and given the fact that no published geochronology constraining the timing of alteration exists for the other two large hematite breccia deposits, Prominent Hill and Carrapateena, it appears that the concept of the Olympic Cu-Au province referred to above may not have been unambiguously validated with respect to this style of IOCG deposit on the eastern Gawler craton.

Here, we report new geochronology from a recently discovered hematite breccia-rich Cu-Au prospect located some 30 km northeast of Olympic Dam—the Vulcan prospect. It (Figs. 1, 2) is known from eight drill holes that penetrate a significant gravity anomaly under the regionally extensive Neoproterozoic cover rocks of the Stuart shelf (Fig. 1). The hematite breccias intersected at Vulcan (Fig. 3a) contain molybdenite intergrown with chalcopyrite. We have dated this molybdenite with the Re-Os method in order to investigate if these hematite breccias and their associated alteration and mineralization can be shown to be temporally coincident with the Gawler Range Volcanics/Hiltaba Suite magmatic event, thereby testing if hematite breccia-related mineralization is part of the early Mesoproterozoic Olympic Cu-Au province. We have also dated one of the breccias that is rich in granitic clasts in order to investigate the age of some of the host rocks to the breccia system at Vulcan.

Geology of the Gawler Craton

The geology of the Gawler craton has been discussed in detail in Daly et al. (1998) and Hand et al. (2007). Archean units of the Gawler craton include ca. 3250 to 3150 Ma (Fraser et al., 2010) and ca. 2555 to 2485 Ma gneiss belts (Fig. 1), which are overlain and intruded by post-2000 Ma sedimentary and magmatic sequences. Granitoids emplaced at ca. 2000 Ma and ca. 1850 Ma form the basement to a series of ca. 2000 to 1740 Ma volcanosedimentary basins (Parker et al., 1993; Fanning et al., 2007; Szpunar et al., 2011). Deposition in the Paleoproterozoic volcanosedimentary sequences was terminated by the ca. 1730 to 1690 Ma Kimban Orogeny (Parker et al., 1993).

Syn- to posttectonic I-type granites were emplaced ca. 1690 to 1670 Ma (Payne et al., 2010), which preceded a series of ca. 1620 to 1608 Ma juvenile bimodal intrusive rocks emplaced in

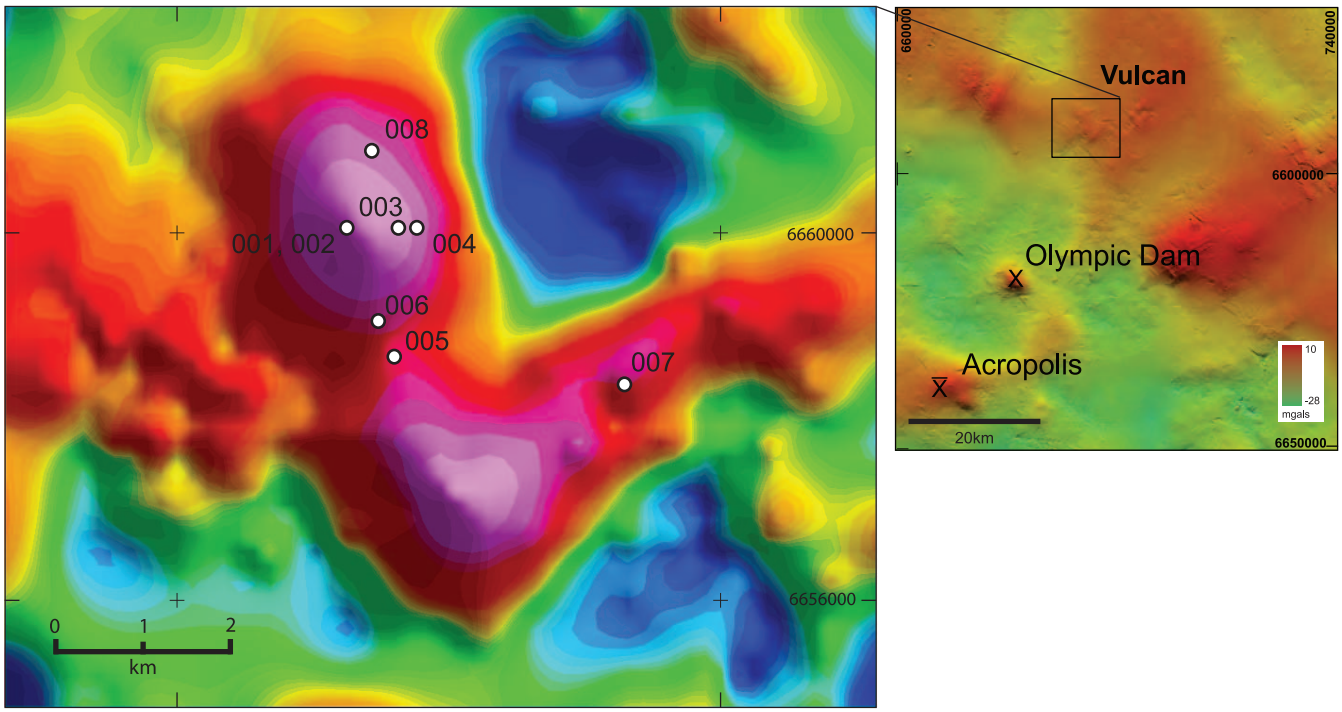

FIG. 2. Pseudocolor residual gravity image over the Vulcan prospect showing the location of Tasman Resources drill holes. The Vulcan gravity anomaly peaks at approximately 2.5 to 3.0 mGal above the regional background. Note that the different drill holes have prefixes that begin with RCDD11VUD, and only the abbreviated drill hole number is shown. Inset shows location of Vulcan relative to Olympic Dam on a regional gravity image (DMITRE data). All coordinates are in GDA 1994 MGA zone 53.

TABLE 1. Summary of Geochronologic Constraints on Timing of

Deposit/prospect	Alteration and sulfide mineral paragenetic stages (numbered)[1]	Reference	Gawler Range Volcanics/ Hiltaba Suite present?
Olympic Dam[2]	1. Mag ± Hem, Chl, Ser, Sd, Py, Ccp, Pt 2. Hem, Ser, Cc, Bn, Py, Brt, Fl, Chl 3. Hem, Qtz, Brt	Oreskes and Einaudi, 1990, 1992; Reeve et al., 1990; Haynes et al., 1995; Johnson and Cross, 1995; Johnson and McCulloch, 1995; Reynolds, 2001; Ehrig, 2010; BHP Billiton Annual Report 2011	Yes
Prominent Hill[2]	1. Ccp, Bn, Cc, Hem, Ser, Qtz 2. Fl, Ur	OZ Minerals Annual Report 2010	Yes
Carrapateena[2]	1. Hem, Ser, Qtz, Ccp, Bn	OZ Minerals Annual Report 2011	None reported
Vulcan[2]	1. Mag ± Hem, Chl, Ser 2. Hem, Ser, Ccp, Bn, Py, Chl, Qtz, Mo	Tasman Resources Annual Reports 2010, 2011	Not confirmed
Oak Dam	1. Mag-Qtz-Ap-Py 2. Colloform Hem 3. Hem after Mag; chalcedony, Qtz-Ill, Chl, Ser, Mnz, Ccp, Py, Sp, Ap, Carb, Ur 4. Vuggy Qtz ± Brt	H.L. Paterson, in Davidson et al., 2007	Not confirmed; felsic dikes may be Hiltaba Suite
Wirrda Well	Mag, Hem, Sid, Qtz, Kfs, Ser, Chl, Bar, Fl, Ap, Bt, Py, Ccp, Bn, Ur		Not confirmed; felsic volcanic rocks may be Gawler Range Volcanics
Hillside	1. Mag, Cpx, Act, Grt, Qtz, Cal, Kfs, Py, Ttn 2. Aln, Ccp, Bn, Hem, Chl, Qtz, Cc	Conor et al., 2010; Rex Minerals Annual Report 2011	Yes
Punt Hill	Mag, Cpx, Grt, Act, Qtz, Kfs, Py, Ttn, Gal, Sp, Ccp, Bn, Hem, Chl, Qtz, Cc	Reid et al., 2011	Yes
Moonta-Wallaroo district	Qtz, Carb, Tur, Ap, Fl, Amph, Cpx, Mag, Kfs, Bt, Py, Po, Ccp 1. Mag, Bt, Alb, Act, Ttn, Tur 2. Qtz, Kfs, Chl, Hem, Mo, Cal, Qtz, Bt, Chl, Ser, Ccp, Py, Mo	Skirrow et al., 2007 Skirrow et al., 2007 Barratt, 1991	Yes
Emmie Bluff	1. Mag, Cpx, Act, Grt, Qtz, Cal, Kfs, Py, Aln 2. Ccp, Bn, Hem, Chl, Qtz, Cc		Yes
Torrens	1. Mag, Qtz, Py, Kfs, Ap, Carb 2. Hem, Chl, Ms/Ser, Ccp	Skirrow et al., 2007	None reported
Murdie Murdie	1. Mag, Alb, Act, Ap, Ttn, Py, Ccp, Carb 2. Kfs 3. Hem, Chl, Cal	Paterson et al., 1986	None reported
Manxman West	1. Alb, Scp, Cpx, Qtz, Act 2. Mag, Bt, Ap, Ttn, REE 3. Po, Ccp, Py, REE-U-Th minerals, Hem, Chl, Cal, Alb, Fl, Kfs, Stp, Brt, Ser	Freeman and Tomkinson, 2010	Yes
Acropolis	Mag, Hem, Ser, Chl, Kfs, Bar, Fl, Ap, Bt, Py, Ccp, Ur	Paterson, 1986	Yes
Titan	1. Bladed Hem 2. Mag, Qtz, Act, Tr, Py, Kfs, Ccp 3. Hem, Carb, Chl	Barrat, 1991	Not confirmed; felsic dikes may be Hiltaba Suite
Joes Dam	Alb, Act, Cpx, Mag, Py, Ccp, Bt, Hem	Freeman and Tomkinson, 2010	None reported

Abbreviations: Act = actinolite, Alb = albite, Aln = allanite, Amph = amphibole, Ap = apatite, Bar and Brt = barite, Bn = bornite, Bt = biotite, Cal = calcite, Carb = carbonate, Cc = chalcocite, Ccp = chalcopyrite, Chl = chlorite, Cpx = clinopyroxene, Fl = fluorite, Gal = galena, Grt = garnet, Hem = hematite, ID-TIMS = isotope dilution-thermal ionization mass spectrometry, Ill = illite, Kfs = K-feldspar, LA-ICP-MS = laser ablation-inductively coupled plasma-mass spectrometry, Mag = magnetite, Mnz = monazite, Mo = molybdenite, Ms = muscovite, NTIMS = negative thermal ionization mass spectrometry, Po = pyrrhotite, Pt = pitchblende, Py = pyrite, Qtz = quartz, Scp = scapolite, Sd and Sid = siderite, Ser = sericite, Sp = sphalerite, Stp = stilpnomelane, Tr = tremolite, Ttn = titanite, Tur = tourmaline, Ur = uraninite

[1] Paragenetic stages after Skirrow et al. (2007), this study, and cited references; mineral abbreviations follow Kretz (1983)

[2] Indicates deposit or prospect is dominated by hematite breccias

Mineralization at Cu-Au Deposits and Prospects, Olympic Cu-Au Province

Age constraint on timing of alteration/mineralization	Dated rock type	Dated minerals	Geochronology method(s)	Mineralization/alteration geochronology reference
1520–ca. 750 Ma	Unknown	Whole rock	Rb-Sr	Reeve et al., 1990
c. 1400 Ma	Unknown	Pitchblende	SHRIMP, U-Pb	Reed et al., 1988
1572 ± 99 Ma	Breccia, granite	Sulfides, whole rock	Sm-Nd	Johnson and McCulloch, 1995
1258 ± 28 Ma	Breccia, granite	Sulfides, whole rock	Re-Os	McInnes et al., 2008
ca. 1400–1200 Ma	Breccia	Sulfides, whole rock	Pb-Pb	Meffre et al., 2010
1597 ± 8 Ma	Ash-fall tuff	Zircon	SHRIMP, U-Pb	Johnson and Cross, 1995
1596 ± 4.4 Ma	Sericitized porphyritic volanic	Zircon	SHRIMP, U-Pb	Jagodzinski, 2005
1585 ± 8 Ma	Porphyritic volanic	Zircon	SHRIMP, U-Pb	C.M. Fanning, pers. comm., in Belperio et al., 2007
No published data				
1586 ± 8 Ma	Hematite breccia	Molybdenite	NTIMS, Re-Os	This study
1455 ± 20 Ma	Altered metasedimentary rock	Monazite	LA-ICP-MS, U-Pb	Davidson et al., 2007
No published data				
1584 ± 6 Ma	Altered metasedimentary rock	Allanite	SHRIMP U-Pb	Gregory et al., 2011
1601 ± 16 Ma	Altered metasedimentary rock	Titanite	SHRIMP U-Pb	Gregory et al., 2011
1586 ± 11 Ma	Altered metasedimentary rock	Titanite	SHRIMP U-Pb	Gregory et al., 2011
1577 ± 7 Ma	Altered metasedimentary rock	Garnet-diopside	Sm-Nd isochron	Reid et al., 2011
1599 ± 6 Ma	Altered metasedimentary and porphyritic volcanic rocks	Molybdenite	Re-Os	Skirrow et al., 2007
1577 ± 6 Ma	Altered metasedimentary and porphyritic volcanic rocks	Molybdenite	Re-Os	Skirrow et al., 2007
1574 ± 6 Ma	Altered metasedimentary and porphyritic volcanic rocks	Molybdenite	Re-Os	Skirrow et al., 2007
No published data				
1575 ± 11 Ma	Altered metasedimentary rock	Muscovite	$^{40}Ar/^{39}Ar$	Skirrow et al., 2007
1576 ± 5 Ma	Altered metasedimentary rock	Titanite	SHRIMP, U-Pb	Skirrow et al., 2007
1567 ± 10 Ma	Altered metasedimentary rock	Titanite	SHRIMP, U-Pb	Skirrow et al., 2007
1604 ± 9 Ma	Altered metasedimentary rock	Apatite	ID-TIMS, U-Pb	Mortimer et al., 1988
No published data				
No published data				

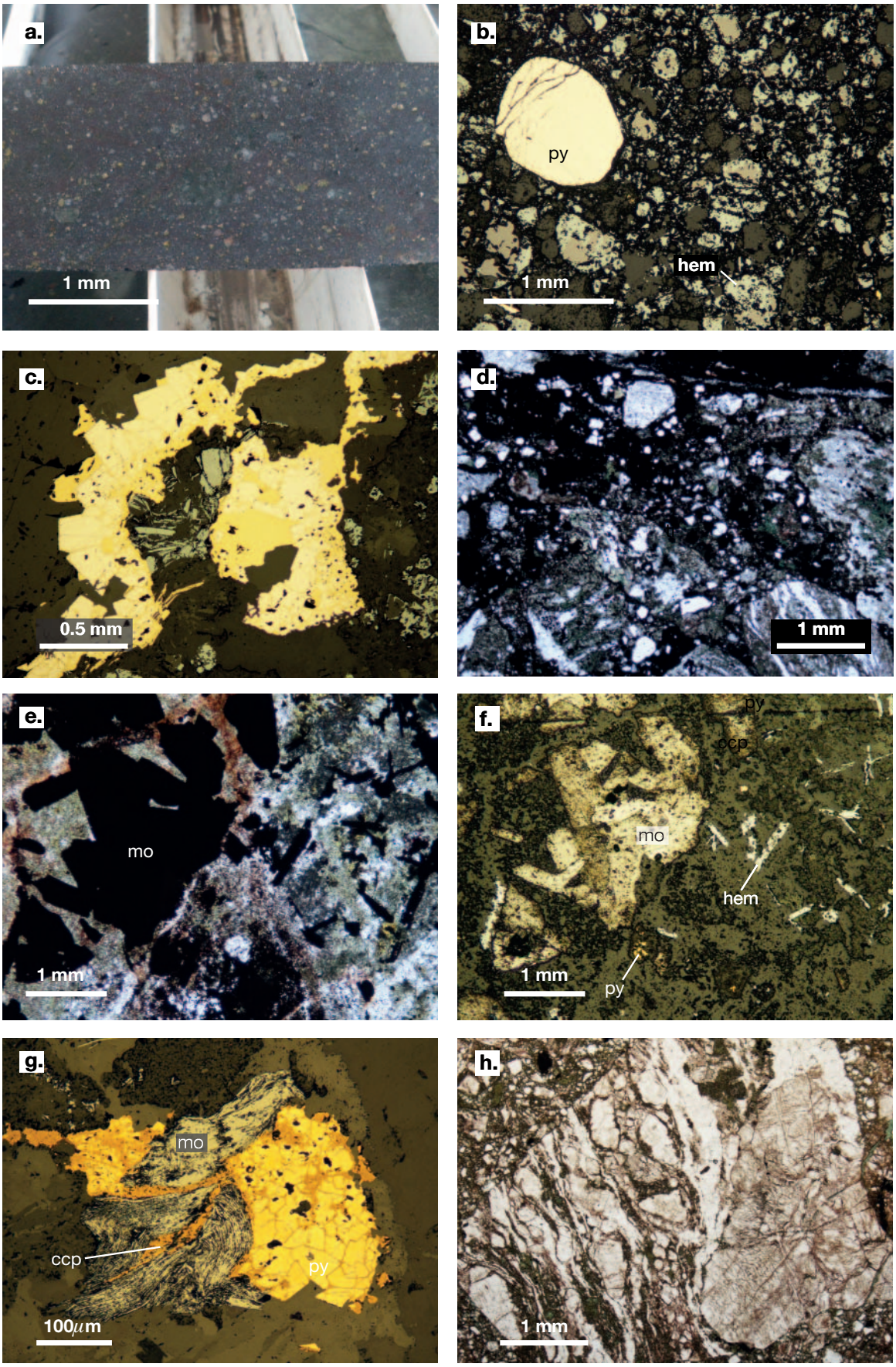
a.
1 mm
b.
py
hem
1 mm
c.
0.5 mm
d.
1 mm
e.
mo
1 mm
f.
py
ccp
mo
hem
1 mm
py
g.
mo
ccp
py
100μm
h.
1 mm

the western Gawler craton (St. Peter Suite; Swain et al., 2008). Voluminous, high-temperature, A-type intrusive and volcanic rocks were formed across much of the Gawler craton between ca. 1600 and 1570 Ma. The extrusive components of this large igneous province, the ca. 1595 to 1587 Ma Gawler Range Volcanics, contain examples of inverted pigeonite indicative of their high temperatures of formation (Blissett et al., 1993) and are part of a major felsic large igneous province (Allen et al., 2008; Pankhurst et al., 2011; Wade et al., 2012). Their intrusive counterpart, the Hiltaba Suite, comprises A-type plutons and includes a regionally distributed mafic component (Flint et al., 1993; Zang et al., 2007).

Localized felsic magmatism at ca. 1500 Ma (Fanning et al., 2007) was followed by ca. 1500 to 1450 Ma low- to moderate-temperature reworking within major shear zones (Fraser and Lyons, 2006). After ca. 1450 Ma, cratonization resulted in a long history of relatively subdued topography as indicated by the numerous sedimentary basins that now cover large portions of the region, including the Neoproterozoic Stuart shelf region of the Adelaide rift complex (Preiss, 2000), which almost entirely covers the basement geology of the Olympic Cu-Au province.

Vulcan Prospect

The Vulcan prospect is a recently discovered hematite breccia-hosted Cu-Au system located approximately 30 km northeast of Olympic Dam (Figs. 1, 2). The prospect is defined by a gravity anomaly and, thus far, only eight diamond drill holes. These drill holes are located mainly on the northern part of the gravity anomaly (Tasman Resources Ltd. data; Fig. 2). All of the drill holes have intersected hematite-rich alteration and Cu-Au ± U mineralization, for example, 57 m at 0.59% Cu, including higher-grade zones such as 0.75 m at 4.44% Cu, 1.34 g/t Au, 0.58 kg/t U_3O_8 and 0.65 m at 7.82% Cu, 2.41 g/t Au within drill hole RCDD10VUD003, and 163-m Cu-Au–mineralized hematite-rich breccias at 0.23% Cu and 0.08 g/t Au within drill hole RCDD11VUD007. Drill hole RCDD11VUD008 intersected 180 m of alteration and mineralization with sulfide mineral zoning from bornite through chalcopyrite to pyrite + chalcopyrite at depth, a zonation pattern similar to that observed at Olympic Dam (Reeve et al., 1990). The gravity and magnetic data for the Vulcan prospect suggest possible continuity of hematite (+ minor magnetite)-altered rock over approximately 12 km^2 (Fig. 2), which is comparable in size to the Olympic Dam deposit, although at a significantly greater depth: ~850 m compared to ~350 m at Olympic Dam. Exploration drilling of the prospect is ongoing.

Mineralization occurs within a variety of breccia types ranging from those that are hematite dominant, composed entirely of hydrothermal minerals (Fig. 3a), to those dominated by altered rock in which clasts of protolith rock are preserved. The highest-grade zones of mineralization at Vulcan occur within hematite-dominant breccias. Hematite breccias comprise a fine-grained hematite-sericite-chlorite–rich matrix that envelops angular to rounded aggregates of quartz, carbonate, sericite, chlorite, pyrite, chalcopyrite ± gold ± apatite ± molybdenite. Iron oxide aggregates within these comprise composite hematite-magnetite granules, with the former enclosing and altering the latter to pseudomorphs (Fig. 3b). Veinlets and larger bodies up to 1 m of coarse to very coarse chalcopyrite and pyrite, which are intergrown with bladed hematite in places (Fig. 3c), are also present. Within the hematite breccia, the overall mineralogy is dominated by smaller, rounded aggregates of altered mylonitic granite and single- and polycrystalline carbonate and single crystal quartz grains (Fig. 3d), and hematite-pyrite-chalcopyrite aggregates occur within a matrix of microcrystalline sericite, chlorite, and carbonate (Fig. 3e). Bladed hematite, coarse-grained pyrite, and chalcopyrite grains are associated with and in places intergrown with coarse-grained laths of molybdenite up to several mm in length (Fig. 3f). Late-stage carbonate veining is common. Carbonate and apatite are also associated with the hematite-rich sulfide aggregates. In places, chlorite forms coarse clots or crosscutting veinlets within the brecciated matrix.

Molybdenite occurs as coarse laths that are intergrown with pyrite and chalcopyrite and also occurs as laths within sericite + chlorite-altered granitic host rocks within each of the samples dated by the Re-Os method (Fig. 3f). Examples of hematite-stained quartz-orthoclase pegmatite and hematite-sericite-chlorite–altered and variably fractured and brecciated mylonitic granite (Fig. 3g) occur within the hematite breccias, and a sample of clast-rich granitic breccia was selected for zircon dating.

Geochronologic Methods

Re-Os geochronology on molybdenite from the Vulcan prospect was performed at the TOTAL Laboratory for Source Rock Geochronology and Geochemistry at Durham University, United Kingdom, using methods identical to those documented in Selby et al. (2007). Molybdenite was isolated from

FIG. 3. Textural features of the Vulcan prospect. a. Typical hematite-dominated breccia. Drill hole RCDD11VUD007, 1,138 m. b. Coarse pyrite granule within hematite-sericite–rich breccia, sample 1838227, drill hole RCDD11VUD007, 1,203.65 m. Note the hematite grains have cores of magnetite (darker gray) and all the grains appear to have been rounded during the brecciation process. Reflected-light image. c. Bladed hematite adjacent to coarse chalcopyrite-pyrite vein. Sample 1836480, drill hole RCDDVUD003, 874.75 m. Reflected-light image. d. Example of hematite-rich breccias with fragments of mylonitic granite, carbonate, and quartz grains, with abundant chlorite-sericite-hematite alteration. Sample 1838227, drill hole RCDD11VUD007, 1,203.65 m. e. Example of intensely sericite altered granitic breccia, showing coarse molybdenite and bladed hematite within the sericite-chlorite–rich matrix. Sample 1836478, drill hole RCDD10VUD002, 1,110 m. Transmitted-light image. f. Reflected-light image of same field of view as (e) showing the molybdenite, hematite, and pyrite assemblage. g. Molybdenite intergrown with pyrite and chalcopyrite within a quartz-sericite matrix. Sample 1836480, drill hole RCDD10VUD003, 874.75 m. Reflected-light image. h. Detail of clast of mylonitic granite within hematite-sericite-chlorite–altered granitic breccia from the sample dated by zircon U-Pb SHRIMP methods. Sample 1838226, drill hole RCDD11VUD007, 1,202.3 m. Transmitted-light image. Abbreviations: ccp = chalcopyrite, hem = hematite, mo = molybdenite, py = pyrite.

cut diamond core surfaces by removing the molybdenite from the rock using a steel probe. Molybdenite was loaded into a Carius tube together with a tracer solution of ^{185}Re and normal Os and a 3:1 mix of HNO_3 and HCl. Os was isolated and purified from the acid solution using solvent extraction ($CHCl_3$) and microdistillation methods. The Re fraction was purified by standard anion chromatography. Both the purified Re and Os fractions were analyzed for their isotope compositions by negative thermal ionization mass spectrometry using Faraday collectors by a Thermo TRITON mass spectrometer. All data are blank corrected (Re = 2 pg; Os = 0.5 pg with an $^{187}Os/^{188}Os$ value of ca. 0.20), although the corrections are insignificant given the high Re and Os abundances of the molybdenite. Uncertainties (Table 2) were determined using the uncertainty in weighing the sample and tracer solution, calibration of the tracer solution, mass spectrometer measurements, and blank values. The Re-Os data with the ^{187}Re decay constant, including its uncertainty (1.666×10^{-11}; Smoliar et al., 1996; Selby et al., 2007), were used to calculate Re-Os model dates. In-house Re and Os (DROsS) solution standards analyzed alongside the sample analysis were 0.59777 ± 0.0015 (n = 2) and 0.16095 ± 0.0004 (n = 2), respectively. These values are in agreement with the running average for the Re standard (0.59772 ± 0.00172, 1 SD, n = 114; Rooney et al., in press) and DROsS Faraday Collector measurements (0.16099 ± 0.0009; n = 10; Selby, unpub. data). The NIST Henderson Reference molybdenite (NIST RM8599) was also analyzed during the course of this study and gave an Re-Os date of 27.7 ± 0.1 Ma (Table 2), which is identical to the reference value (Markey et al., 2007).

Zircon U-Pb geochronology was undertaken at the Geoscience Australia geochronology laboratory, Canberra, using SHRIMP IIe instrumentation. Zircon was extracted via standard crushing, density, and magnetic separation procedures. Zircon grains were then encapsulated in epoxy, together with the multigrain zircon standards OG1 and Temora 2. Zircon standard M257 (840 ppm U) was also mounted and used as a U concentration standard. The mounts were polished to expose grains in section. All grains were photographed in transmitted and reflected light, and imaged by cathodoluminescence. Isotopic data were collected using a primary oxygen ion beam of ~2- to 2.5-nA intensity and ~20-μm diameter. Differential fractionation between U and Pb and isobaric interference at the ^{204}Pb mass peak were monitored by reference to a $^{206}Pb/^{238}U$ ratio of 0.0668 for interspersed analyses of the 416.8 ± 0.3 Ma Temora 2 zircon standard (Black et al., 2003). The OG1 standard (Stern et al., 2009) was used to monitor $^{207}Pb/^{206}Pb$ reproducibility and accuracy. Radiogenic Pb compositions were determined by subtracting contemporaneous nonradiogenic Pb (Stacey and Kramers, 1975). U-Pb data were processed using SQUID 2 (Ludwig, 2009) and plotted using ISOPLOT/EX 3.71 (Ludwig, 2003), using the U and Th decay constants of Jaffey et al. (1971), as recommended by Steiger and Jäger (1977). Uncertainties are quoted at the 95% confidence level.

Geochronology Results

The Re-Os dating produced a tight cluster of ages at ca. 1587 Ma (Table 2). A well-fitting ^{187}Re vs. ^{187}Os isochron produces an age of 1590 ± 12 Ma (MSWD = 0.113; Fig. 4). This isochron produces an initial ^{187}Os value within uncertainty of zero (7 ± 47), indicating all ^{187}Os is radiogenic in origin. A weighted mean age derived from the four analyses yields an age of 1586 ± 3 Ma (2σ; MSWD = 0.18), which we interpret to be the best estimate of the timing of crystallization of molybdenite at Vulcan. If the uncertainties are augmented to account for uncertainty in the ^{187}Re decay constant of 0.31% (Selby et al., 2007), the uncertainty for the weighted mean age becomes 8 m.y., which should be quoted when comparing these Re-Os ages to other isotope systems.

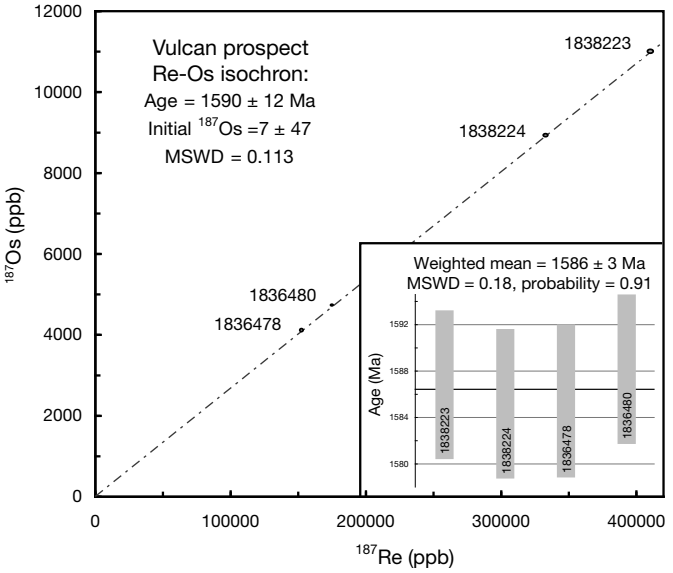

FIG. 4. ^{187}Re vs. ^{187}Os diagram for samples from the Vulcan prospect. Inset shows weighted mean age calculation.

TABLE 2. Summary of Molybdenite Re-Os Isotope Data from Vulcan Prospect

Sample no.	Drill hole	Depth (m)	Wt (mg)	Re (ppm)	±	^{187}Re (ppm)	±	^{187}Os (ppb)	±	Age (Ma)	±2σ	±2σ[1]
1838223	RCDD09VUD001	1,019.10–1,019.20	0.018	653.3	2.5	410.6	1.6	10,999.3	36.6	1586.8	6.4	8.1
1838224	RCDD09VUD001	1,029.00–1,029.06	0.018	530.6	2.1	333.5	1.3	8,925.0	29.9	1585.2	6.4	8.2
1836478	RCDD10VUD002	1,110.10–1,110.05	0.006	243.0	1.9	152.7	1.2	4,088.0	30.4	1585.4	6.6	8.3
1836480	RCDD10VUD003	874.75–874.95	0.021	279.1	1.0	175.4	0.7	4,702.7	14.7	1588.2	6.4	8.2
RO393-5 RM8599[2]			0.102	11.032	0.035	6.934	0.02	3.2	0.008	27.72	0.11	0.14

[1] Includes uncertainty associated with ^{187}Re decay constant
[2] Reference molybdenite; reference values reported in Markey et al. (2007)

SHRIMP zircon dating was undertaken on zircon from sample 1838226, a hematite-altered, sericite-rich breccia that comprises clasts of both foliated granite within a matrix of brecciated K-feldspar, and plagioclase and quartz grains (Fig. 3g). This granitic breccia sample occurs as a zone 1.5 m in width, within a broader zone of more hematite dominated breccia in which the hematite is the dominant mineral and the granitic portion of the breccia is less. Only 13 zircon grains, which are clear to light brown and show oscillatory zonation typical of igneous zircon under cathodoluminesence, were recovered from the 40-cm ¼ core sample (Fig. 5). Thirteen analyses were made on these 13 zircon grains, and all but two are concordant or near concordant and cluster at ca. 1745 Ma (Table 3; Fig. 5). The two discordant grains lie on a discordia trend with the near-concordant data that define an upper intercept of 1748 ± 7 Ma and a lower intercept of 546 ± 91 Ma (MSWD = 0.94; Fig. 5). The weighted mean $^{207}Pb/^{206}Pb$ age of those grains that are concordant yields an age of 1743 ± 7 Ma (n = 11; MSWD = 1.5; probability = 0.13), which is interpreted as the best estimate for the timing of crystallization of the granitic rock now incorporated within the hematite breccia. The nonzero age lower intercept suggests this zircon underwent radiogenic Pb loss in the late Neoproterozoic.

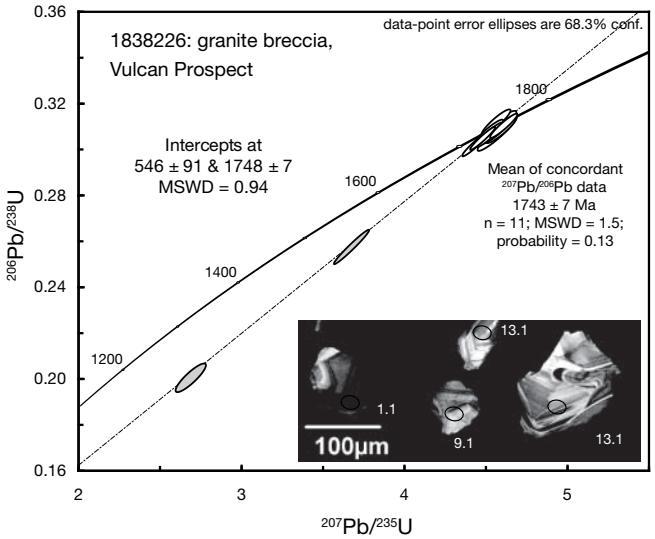

FIG. 5. Summary of SHRIMP U-Pb zircon data from sample 1838226, granite breccia, Vulcan prospect. Inset shows cathodoluminescence image of zircon from this sample.

Discussion

Timing of molybdenite crystallization at Vulcan and implications for the Olympic Cu-Au province

Our new Re-Os molybdenite data from Vulcan link this hematite breccia-rich Cu-Au occurrence to the other Cu-Au deposits across the region. Because the molybdenite at Vulcan is intergrown with chalcopyrite within altered granite breccia and hematite-rich, matrix-supported breccia, it can be considered to have formed synchronously with the primary mineralizing event at Vulcan. Based on these textural observations, the new Re-Os data from Vulcan demonstrate that hydrothermal activity and mineralization occurred at 1586 ± 8 Ma. Therefore, we concur with the majority of previous studies in suggesting that the most reasonable interpretation of the rock relationships and regional geology of the hematite-dominant breccia systems of the eastern Gawler craton is that they formed between ca. 1594 and ca. 1575 Ma and are therefore temporally associated with the Gawler Range Volcanics/Hiltaba Suite magmatic event.

In light of the molybdenite age for Vulcan, we suggest that the range of isotopic ages returned from different studies at Olympic Dam may reflect a younger disturbance or series of disturbances through fluid flow, paleoweathering, or groundwater processes, perhaps enhanced by the highly uraniferous nature of the Olympic Dam orebody itself. Isotopic disturbance is also evident in our zircon U-Pb data from the granite breccia of the Vulcan prospect and in at least one other prospect from the region (Oak Dam; Davidson et al., 2007).

Age of granitic protolith

The granitic protolith dated at Vulcan at 1743 ± 7 Ma may be related to ca. 1750 to 1740 Ma intrusive and extrusive magmatism documented from a number of localities in the eastern Gawler craton, including the Moonta Porphyry (1748 ± 15 Ma; Fanning et al., 2007), unnamed granite gneiss in the north-central Eyre Peninsula (sample 445506, 1740 ± 4 Ma; Fanning et al., 2007), and the less well constrained Burkitt Granite (1742 ± 42 Ma; Fraser and Neumann, 2010). Felsic

TABLE 3. Summary of Zircon U-Pb SHRIMP Data from Sample 1838226, Vulcan Prospect

Spot	U (ppm)	Th (ppm)	Th/U	$^{206}Pb_c$ (%)	$^{206}Pb^*$ (ppm)	$^{206}Pb^*/^{238}U$	± %	$^{207}Pb^*/^{235}U$	± %	$^{207}Pb^*/^{206}Pb^*$	± %	$^{207}Pb/^{206}Pb$ Age (Ma)	±	disc (%)
226.2.1.1	51	21	0.43	0.07	9	0.201	2.0	2.68	2.3	0.0966	1.1	1559	21	26
226.4.1.1	259	99	0.40	0.11	57	0.258	1.9	3.67	2.0	0.1031	0.4	1680	8	13
226.11.1.1	135	57	0.44	0.06	36	0.312	1.2	4.56	1.3	0.1059	0.5	1729	10	–1
226.1.1.1	279	103	0.38	–0.03	73	0.302	1.1	4.43	1.2	0.1061	0.4	1734	7	2
226.12.1.1	144	39	0.28	0.03	38	0.308	1.2	4.51	1.3	0.1063	0.5	1736	9	0
226.10.1.1	323	143	0.46	0.03	85	0.305	1.1	4.47	1.1	0.1063	0.3	1737	6	1
226.7.1.1	277	98	0.37	0.01	73	0.308	1.3	4.53	1.3	0.1066	0.3	1742	6	1
226.8.1.1	172	79	0.47	0.07	45	0.307	1.2	4.52	1.2	0.1067	0.5	1745	8	1
226.6.1.1	94	60	0.66	–0.08	25	0.311	1.3	4.58	1.4	0.1068	0.7	1745	12	0
226.3.1.1	135	57	0.44	0.08	36	0.309	1.2	4.56	1.3	0.1071	0.5	1751	10	1
226.5.1.1	181	80	0.46	–0.01	48	0.311	1.1	4.60	1.2	0.1075	0.4	1757	8	1
226.9.1.1	142	67	0.48	0.20	38	0.307	1.6	4.56	1.8	0.1076	0.6	1760	11	2
226.13.1.1	124	73	0.61	–0.04	33	0.309	1.2	4.59	1.3	0.1077	0.5	1761	10	2

and mafic volcanic rocks with ages ca. 1750 to 1740 Ma are documented from the southern Gawler craton, where they are intercalated with siliciclastic sediments (e.g., Wallaroo Group; Fanning et al., 1988, 2007; Fraser and Neumann, 2010), and are part of a period of widespread sedimentation across the Gawler craton (Daly et al., 1998; Hand et al., 2007). The mylonitic nature of the granite at Vulcan, as evidenced within the larger granitic clasts within sample 1838226, suggests that the region underwent some degree of deformation post-ca. 1743 Ma, although the timing of this remains unconstrained at present.

These new granite age data further indicate the diversity in ages of basement rocks that are host to Gawler Range Volcanics/Hiltaba Suite-related Cu-Au ± U mineralization within the region. Mineralization at Olympic Dam is hosted predominantly by ca. 1590 Ma igneous rocks and associated sedimentary rocks whereas, at Prominent Hill, the host rocks are ca. 1590 Ma volcanosedimentary sequences (Belperio et al., 2007). In contrast, at the Hillside deposit, the host rocks are ca. 1750 Ma volcanosedimentary rocks and ca. 1600 Ma granites (Gregory et al., 2011), similar to other deposits in the Moonta-Wallaroo district (Skirrow et al., 2007), while at Carrapateena the host rock includes ca. 1850 Ma granite (Jagodzinski et al., 2007; Porter, 2010). It appears, therefore, that the host-rock age is a less significant determinant of the presence of mineralization within the region, with structural controls on fluid flow being one of the most critical factors (Hayward and Skirrow, 2010).

Conclusions

Recent drilling into a gravity anomaly at the Vulcan prospect has revealed that hematite-rich brecciation and hematite + sericite + chlorite alteration is associated with Cu-Au mineralization. Re-Os dating of molybdenite intergrown with pyrite and chalcopyrite yields a weighted mean age of 1586 ± 8 Ma (2σ; MSWD = 0.18, including decay constant errors). A sample of brecciated granite returned a SHRIMP zircon U-Pb crystallization age of 1743 ± 7 Ma. This age is different from those of other host rocks known from the Stuart shelf region, highlighting the diversity in host rock ages between the different deposits and prospects. The molybdenite Re-Os data yield an unambiguous date of the timing of Cu-Au mineralization and related hematite brecciation at Vulcan and indicate it formed as part of the same broad, early Mesoproterozoic mineralizing event in which other deposits and prospects of the Olympic Cu-Au province also formed (Skirrow et al., 2007).

Acknowledgments

Massimo Chiaradia provided a helpful review of this manuscript. Mike Harris and Ross Large provided helpful comments on earlier versions. The SHRIMP geochronology presented here is part of a National Geoscience Agreement between Geoscience Australia and DMITRE. AR and EJ publish with permission of the director, Geological Survey of South Australia. RS publishes with permission of the chief executive officer, Geoscience Australia.

REFERENCES

Allen, S.R., McPhie, J., Ferris, G., and Cadd, A.G., 2008, Evolution and architecture of a large felsic igneous province in western Laurentia: The 1.6 Ga Gawler Range Volcanics, South Australia: Journal of Volcanology and Geothermal Research, v. 172, p. 132–147.

Barratt, R.M., 1991, Stuart Shelf Project. EL 1338 first partial relinquishment report for the period 2/5/1975 to 16/6/1991: South Australia Department of Primary Industries and Resources, Open File Envelope 08482, 609 p.

Bastrakov, E.N., Skirrow, R.G., and Davidson, G.J., 2007, Fluid evolution and origins of iron oxide Cu-Au prospects in the Olympic Dam district, Gawler craton, South Australia: Economic Geology, v. 102, p. 1415–1440.

Belperio, A., Flint, R., and Freeman, H., 2007, Prominent Hill: A hematite-dominated, iron oxide copper-gold system: Economic Geology, v. 102, p. 1499–1510.

BHP Billiton, 2011, 2011 Annual Report: BHP Billiton, 268 p., available online at <http://www.bhpbilliton.com/home/investors/reports/Documents/2011/2011AnnualReport.pdf>.

Black, L.P., Kamo, S.L., Williams, I.S., Mundil, R., Davis, D.W., Korsch, R.J., and Foudoulis, C., 2003, The application of SHRIMP to Phanerozoic geochronology; a critical appraisal of four zircon standards: Chemical Geology, v. 200, p. 171–188.

Blissett, A.H., Creaser, R.A., Daly, S., Flint, D.J., and Parker, A.J., 1993, Gawler Range Volcanics: Adelaide, Geological Survey of South Australia Bulletin 54, p. 107–131.

Conor, C.C.H., Raymond, O., Baker, T., Teale, G.S., Say, P., and Lowe, G., 2010, Alteration and mineralisation in the Moonta-Wallaroo copper-gold mining field region, Olympic Domain, South Australia, *in* Porter, T.M., ed., Hydrothermal iron oxide copper-gold & related deposits: A global perspective, v. 3—Advances in the understanding of IOCG deposits: Adelaide, PGC Publishing, p. 1–24.

Daly, S.J., Fanning, C.M., and Fairclough, M.C., 1998, Tectonic evolution and exploration potential of the Gawler craton, South Australia: AGSO Journal of Australian Geology & Geophysics, v. 17, p. 145–168.

Davidson, G.J., Paterson, H., Meffre, S., and Berry, R.F., 2007, Characteristics and origin of the Oak Dam East breccia-hosted, iron oxide Cu-U-(Au) deposit: Olympic Dam region, Gawler craton, South Australia: Economic Geology, v. 102, p. 1471–1498.

Ehrig, K., 2010, Olympic Dam: 35 years since discovery, 2.3 million metres of diamond core, and new (?) ideas: International Association on the Genesis of Ore Deposits (IAGOD), Conference Proceedings of the 13th Quadrennial IAGOD Symposium, Adelaide, South Australia, 6–9 April, 2010, p. 9–10.

Fairclough, M.C., Schwarz, M.P., and Ferris, G.M., 2003, Interpreted crystalline basement geology of the Gawler craton: Adelaide, South Australian Geological Survey, Special Map, 1:1000000 series.

Fanning, C.M., Flint, R.B., Parker, A.J., Ludwig, K.R., and Blissett, A.H., 1988, Refined Proterozoic evolution of the Gawler craton, South Australia, through U-Pb zircon geochronology: Precambrian Research, v. 40–41, p. 363–386.

Fanning, C.M., Reid, A.J., and Teale, G., 2007, A geochronological framework for the Gawler craton, South Australia: South Australia Geological Survey Bulletin 55, p. 258.

Flint, R.B., Blissett, A.H., Conor, C.H.H., Cowley, W.M., Cross, K.C., Creaser, R.A., Daly, S.J., Krieg, G.W., Major, R.B., Teale, G.S., and Parker, A.J., 1993, Mesoproterozoic: Adelaide, Geological Survey of South Australia Bulletin 54, p. 106–169.

Fraser, G., and Lyons, P., 2006, Timing of Mesoproterozoic tectonic activity in the northwestern Gawler craton constrained by $^{40}Ar/^{39}Ar$ geochronology: Precambrian Research, v. 151, p. 160–184.

Fraser, G.L., and Neumann, N., 2010, New SHRIMP U-Pb zircon ages from the Gawler craton and Curnamona province, South Australia, 2008–2010: Geoscience Australia Record 2010/16, p. 256.

Fraser, G., McAvaney, S., Neumann, N., Szpunar, M., and Reid, A., 2010, Discovery of early Mesoarchean crust in the eastern Gawler craton, South Australia: Precambrian Research, v. 179, p. 1–21.

Freeman, H., and Tomkinson, M., 2010, Geological setting of iron oxide related mineralisation in the southern Mount Woods Domain, South Australia, *in* Porter, T.M., ed., Hydrothermal iron oxide copper-gold & related deposits: A global perspective, v. 3—Advances in the understanding of IOCG deposits: Adelaide, PGC Publishing, p. 171–190.

Gow, P.A., Wall, V.J., Oliver, N.H.S., and Valenta, R.K., 1994, Proterozoic iron oxide (Cu-U-Au-REE) deposits: Further evidence of hydrothermal origin: Geology, v. 22, p. 633–636.

Gregory, C.J., Reid, A.J., Teale, G., and Say, P., 2011, U-Pb geochronology of hydrothermal allanite and titanite and magmatic zircon from the Hillside Cu-Au deposit, Yorke Peninsula: South Australia, Department of Primary Industries and Resources Report Book 2011/00003, p. 95–126.

Hand, M., Reid, A., and Jagodzinski, E., 2007, Tectonic framework and evolution of the Gawler craton, South Australia: Economic Geology, v. 102, p. 1377–1395.

Haynes, D.W., Cross, K.C., Bills, R.T., and Reed, M.H., 1995, Olympic Dam ore genesis; a fluid-mixing model: Economic Geology, v. 90, p. 281–307.

Hayward, N., and Skirrow, R., 2010, Geodynamic setting and controls on iron oxide Cu-Au (±U) ore in the Gawler craton, South Australia, *in* Porter, T.M., ed., Hydrothermal iron oxide copper-gold and related deposits: A global perspective, volume 3, advances in the understanding of IOCG deposits: Adelaide, PGC Publishing, p. 105–131.

Jaffey, A.H., Flynn, K.F., Glendenin, L.E., Bentley, W.C., and Essling, A.M., 1971, Precision measurement of half-lives and specific activities of ^{235}U and ^{238}U: Physical Reviews C, v. 4, p. 1889–1906.

Jagodzinski, E.A., 2005, Compilation of SHRIMP U-Pb geochronological data, Olympic Domain, Gawler craton, South Australia, 2001–2003: Geoscience Australia Record 2005/20, p. 211.

Jagodzinski, E.A., Reid, A.J., Chalmers, N.C., Swain, G., Frew, R.A., and Foudoulis, C., 2007, Compilation of SHRIMP U-Pb geochronological data for the Gawler craton, South Australia, 2007: South Australia, Department of Primary Industries and Resources Report Book 2007/21, p. 93.

Johnson, J.P., 1993, The geochronology and radiogenic isotope systematics of the Olympic Dam copper-uranium-gold-silver deposit, South Australia: Unpublished Ph.D. thesis, Canberra, The Australian National University, 251 p.

Johnson, J.P., and Cross, K.C., 1995, U-Pb geochronological constraints on the genesis of the Olympic Dam Cu-U-Au-Ag deposit, South Australia: Economic Geology, v. 90, p. 1046–1063.

Johnson, J.P., and McCulloch, M.T., 1995, Sources of mineralising fluids for the Olympic Dam deposit (South Australia); Sm-Nd isotopic constraints: Chemical Geology, v. 121, p. 177–199.

Kretz, R., 1983, Symbols for rock-forming minerals: American Mineralogist, v. 68, p. 277–279.

Ludwig, K.R., 2003, Isoplot 3.00—a geochronological toolkit for Microsoft Excel: Berkeley Geochronology Center Special Publication no. 4, p. 75.

——2009, SQUID 2.50: A user's manual: Berkeley California, USA, Berkeley Geochronology Center Special Publication no. 5, p. 110.

Markey, R., Stein, H.J., Hannah, J.L., Zimmerman, A., Selby, D., and Creaser, R.A., 2007, Standardizing Re-Os geochronology: A new molybdenite Reference Material (Henderson, USA) and the stoichiometry of Os salts: Chemical Geology, v. 244, p. 74–87.

McInnes, B.I.A., Keays, R.R., Lambert, D.D., Hellstrom, J., and Allwood, J. S., 2008, Re-Os geochronology and isotope systematics of the Tanami, Tennant Creek and Olympic Dam Cu-Au deposits: Australian Journal of Earth Sciences, v. 55, p. 967–981.

McPhie, J., Kamenetsky, V.S., Chambefort, I., Ehrig, K., and Green, N., 2011, Origin of the supergiant Olympic Dam Cu-U-Au-Ag deposit, South Australia: Was a sedimentary basin involved?: Geology, v. 39, p. 795–798.

Meffre, S., Ehrig, K., Kamenetsky, V., Chambefort, I., Maas, R., and McPhie, J., 2010, Pb isotopes at Olympic Dam: Constraining sulphide growth: International Association on the Genesis of Ore Deposits (IAGOD), Conference Proceedings of the 13th Quadrennial IAGOD Symposium, Adelaide, South Australia, 6–9 April, 2010, p. 78–79.

Mortimer, G.E., Cooper, J.A., Paterson, H.L., Cross, K., Hudson, G.R.T., and Uppill, R.K., 1988, Zircon U-Pb dating in the vicinity of Olympic Dam Cu-U-Au deposit, Roxby Downs, South Australia: Economic Geology, v. 83, p. 694–709.

Oreskes, N., and Einaudi, M.T., 1990, Origin of rare earth element-enriched hematite breccias at the Olympic Dam Cu-U-Au-Ag deposit, Roxby Downs, South Australia: Economic Geology, v. 85, p. 1–28.

——1992, Origin of hydrothermal fluids at Olympic Dam: Preliminary results from fluid inclusions and stable isotopes: Economic Geology, v. 87, p. 64–90.

OZ Minerals, 2010, Annual Report 2010: OZ Minerals, 104 p., available online at <http://www.ozminerals.com/Media/docs/ASX_20110414_annual_report2010-d4eb944f-8475-46f7-9951-df97d43628de-0.pdf>.

——2011, Annual Report 2011: OZ Minerals, 108 p., available online at <http://www.ozminerals.com/Media/docs/ASX-20120424-OZ-annual-report-2011-23afee15-7e6b-4e1b-911c-6cdac8075378-0.pdf>.

Pankhurst, M.J., Schaefer, B.F., Betts, P.G., Phillips, N., and Hand, M., 2011, A Mesoproterozoic continental flood rhyolite province, the Gawler Ranges, Australia: The end member example of the large igneous province clan: Solid Earth, v. 2, p. 25–33.

Parker, A.J., Daly, S.J., Flint, D.J., Flint, R.B., Preiss, W.V., and Teale, G.S., 1993, Palaeoproterozoic: Adelaide, South Australia, Geological Survey of South Australia Bulletin 54, p. 50–105.

Paterson, H.L., 1986, The Acropolis Project, *in* Paterson, H.L., Dalgarno, C.R., Esdale, D.J., and Tonkin, D., eds., Excursion A1—Basement geology of the Stuart shelf region, South Australia: South Australia Department of Primary Industries and Resources, Report Book 86/51, p. 27.

Paterson, H.L., Muir, P.M., Uppill, R.K., Hinde, J.S., Arden, P.J., 1986, Andamooka, Stuart Creek, Arcoona, Lake Torrens, Todds Dam, Lake Arthur, Woodforde Hill and Murdie Island (the Stuart Shelf Project). Joint first partial relinquishment report at licences' expiry/renewal, for the period 2/5/1975 to 16/6/1986: South Australia Department of Primary Industries and Resources Open File Envelope 06562, p. 1969.

Payne, J.L., Ferris, G., Barovich, K.M., and Hand, M., 2010, Pitfalls of classifying ancient magmatic suites with tectonic discrimination diagrams: An example from the Paleoproterozoic Tunkillia Suite, southern Australia: Precambrian Research, v. 177, p. 227–240.

Porter, T.M., 2010, The Carrapateena iron oxide copper gold deposit, Gawler craton, South Australia: A review, *in* Porter, T.M., ed., Hydrothermal iron oxide copper-gold & related deposits: A global perspective, v. 3—advances in the understanding of IOCG Deposits: Adelaide, PGC Publishing, p. 191–200.

Preiss, W.V., 2000, The Adelaide Geosyncline of South Australia and its significance in Neoproterozoic continental reconstruction: Precambrian Research, v. 100, p. 21–63.

Reed, S.J.B., Trueman, N.A., and Long, J.V.P., 1988, Ion microprobe U-Pb dating of pitchblende, *in* Benninghoven, A., Huber, A.M., and Werner, H.W., eds., Secondary ion mass spectrometry: SIMS VI: Proceedings of the Sixth International Conference on Secondary Ion Mass Spectrometry (SIMS VI), Palais des Congrès, Versailles, Paris, France, September 13–18, 1987, p. 945–948.

Reeve, J.S., Cross, K.C., Smith, R.N., and Oreskes, N., 1990, Olympic Dam copper-uranium-gold-silver deposit: Australasian Institute of Mining and Metallurgy Monograph 14, p. 1009–1035.

Reid, A.J., Swain, G.S., Mason, D., and Maas, R., 2011, Nature and timing of Cu-Au-Zn-Pb mineralisation at Punt Hill, eastern Gawler craton: MESA Journal, v. 60, p. 7–17.

Rex Minerals Ltd, 2011, Annual Report 2011: Rex Minerals Ltd, 68 p., available online at <http://www.rexminerals.com.au/wp-content/uploads/2010/10/20110922-Rex-Annual-Report-Final1.pdf >.

Reynolds, L.J., 2001, Geology of the Olympic Dam Cu-U-Au-Ag-REE deposit: MESA Journal, v. 23, p. 4–11.

Rooney, A.D., Selby, D., Lewan, M., Lillis, P., and Houzay, J.P., in press, Evaluating Re-Os systematics in organic-rich sedimentary rocks in response to petroleum generation using hydrous pyrolysis experiments: Geochimica et Cosmochimica Acta.

Selby, D., Creaser, R.A., Stein, H.J., Markey, R.J., and Hannah, J.L., 2007, Assessment of the ^{187}Re decay constant by cross calibration of Re-Os molybdenite and U-Pb zircon chronometers in magmatic ore systems: Geochimica et Cosmochimica Acta, v. 71, p. 1999–2013.

Skirrow, R.G., Bastrakov, E., Davidson, G., Raymond, O.L., and Heithersay, P., 2002, The geological framework, distribution and controls of Fe-oxide and related alteration, and Cu-Au mineralisation in the Gawler craton, South Australia. Part II: Alteration and mineralisation, *in* Porter, T.M., ed., Hydrothermal iron oxide copper-gold and related deposits: A global perspective, 2: Adelaide, PGC Publishing, p. 33–47.

Skirrow, R.G., Bastrakov, E.N., Barovich, K., Fraser, G.L., Creaser, R.A., Fanning, C.M., Raymond, O.L., and Davidson, G.J., 2007, Timing of iron oxide Cu-Au-(U) hydrothermal activity and Nd isotope constraints on metal sources in the Gawler craton, South Australia: Economic Geology, v. 102, p. 1441–1470.

Smoliar, M.I., Walker, R.J., and Morgan, J.W., 1996, Re-Os Ages of Group IIA, IIIA, IVA, and IVB iron meteorites: Science, v. 271, p. 1099–1102.

Stacey, J.S., and Kramers, J.D., 1975, Approximation of terrestrial lead isotope evolution by a two-stage model: Earth and Planetary Science Letters, v. 26, p. 207–221.

Steiger, R.H., and Jäger, E., 1977, Subcommission of geochronology: Convention on the use of decay constants in geo- and cosmochronology: Earth and Planetary Science Letters, v. 36, p. 359–362.

Stern, R.A., Bodorkos, S., Kamo, S.L., Hickman, A.H., and Corfu, F., 2009, Measurement of SIMS instrumental mass fractionation of Pb isotopes during zircon dating: Geostandards and Geoanalytical Research, v. 33, p. 145–168.

Swain, G., Barovich, K., Hand, M., Ferris, G., and Schwarz, M., 2008, Petrogenesis of the St Peter Suite, southern Australia: Arc magmatism and Proterozoic crustal growth of the South Australian craton: Precambrian Research, v. 166, p. 283–296.

Szpunar, M., Hand, M., Barovich, K., Belousova, E., and Jagodzinski, E.A., 2011, Isotopic and geochemical constraints on the Paleoproterozoic Hutchison Group, southern Australia: Implications for Paleoproterozoic continental reconstructions: Precambrian Research, v. 187, p. 99–126.

Tasman Resources Ltd., 2010, Annual Report 2010: Tasman Resources Ltd., 47 p.

——2011, Annual Report 2011: Tasman Resources Ltd., 46 p.

Wade, C.E., Reid, A.J., Wingate, M.T.D., Jagodzinski, E.A., and Barovich, K., 2012, Geochemistry and geochronology of the c. 1585 Ma Benagerie Volcanic Suite, southern Australia: Relationship to the Gawler Range Volcanics and implications for the petrogenesis of a Mesoproterozoic silicic large igneous province: Precambrian Research, v. 206–207, p. 17–35.

Zang, W., Fanning, C.M., Purvis, A.C., Raymond, O.L., and Both, R.A., 2007, Early Mesoproterozoic bimodal plutonism in the southeastern Gawler craton, South Australia: Australian Journal of Earth Sciences, v. 54, p. 661–674.